J. Korean Math. Soc. **58** (2021), No. 3, pp. 723–740
https://doi.org/10.4134/JKMS.j200226
pISSN: 0304-9914 / eISSN: 2234-3008

ESTIMATION ALGORITHM FOR PHYSICAL PARAMETERS IN A SHALLOW ARCH

Semion Gutman, Junhong Ha, and Sudeok Shon

Abstract. Design and maintenance of large span roof structures require an analysis of their static and dynamic behavior depending on the physical parameters defining the structures. Therefore, it is highly desirable to estimate the parameters from observations of the system. In this paper we study the parameter estimation problem for damped shallow arches. We discuss both symmetric and non-symmetric shapes and loads, and provide theoretical and numerical studies of the model behavior.

Our study of the behavior of such structures shows that it is greatly affected by the existence of critical parameters. A small change in such parameters causes a significant change in the model behavior. The presence of the critical parameters makes it challenging to obtain good estimation. We overcome this difficulty by presenting the Parameter Estimation Algorithm that identifies the unknown parameters sequentially. It is shown numerically that the algorithm achieves a successful parameter estimation for models defined by arbitrary parameters, including the critical ones.

1. Introduction

Design of large span roof structures requires an analysis of static and dynamic behavior of shallow arches under various loads. There are several mathematical models for such arches [3, 9, 10]. These models differ in the damping effects that are accounted for. Even more general mathematical models are presented in [2] and [5].

In this paper we consider parameter estimation in an arch model with air damping. Let a shallow arch be positioned over the interval $[0, \pi]$. Suppose that it is subjected to the load $p = p(x, t)$, under which it takes the shape $y = y(x, t)$ for $x \in [0, \pi]$, $t > 0$. Let $u_0 = u_0(x)$ be its initial load–free shape. Then the deflection $y = y(x, t)$ of the arch, accounting for a weak damping

Received April 29, 2020; Accepted August 31, 2020.
2010 *Mathematics Subject Classification.* Primary 45M10, 74H55, 65Y10.
Key words and phrases. Shallow arch, parameter estimation, critical pairs, stability analysis, damping effect.
This research was supported by Basic Science Research Program through the National Research Foundation of Korea (NRF) funded by the Ministry of Science and ICT (NRF-2019R1F1A1058327).

effect, is described by the dimensionless nonlinear partial differential equation

$$\frac{\partial^2 y}{\partial t^2} + \frac{\partial^4 y}{\partial x^4} - \left[\beta + \frac{1}{2\pi}\int_0^\pi \left(\frac{\partial y}{\partial x}\right)^2 dx\right]\frac{\partial^2 y}{\partial x^2} + \gamma\frac{\partial y}{\partial t} = f, \tag{1}$$

where

$$\beta = -\frac{1}{2\pi}\int_0^\pi \left(\frac{\partial u_0}{\partial x}\right)^2 dx, \quad f = \frac{\partial^4 u_0}{\partial x^4} + p.$$

Hinged boundary conditions are given by

$$y(0,t) = y(\pi,t) = \frac{\partial^2 y}{\partial x^2}(0,t) = \frac{\partial^2 y}{\partial x^2}(\pi,t) = 0, \quad t \geq 0, \tag{2}$$

and the initial conditions are

$$y(x,0) = u_0(x), \quad \frac{\partial y}{\partial t}(x,0) = v_0(x), \quad x \in [0,\pi]. \tag{3}$$

Model (1)-(3) has attracted a lot of interest because of its engineering importance for real world arch structures, and rich global dynamic behavior of its solutions exhibiting chaotic motion, and various resonance phenomena. There are many research papers on the subject. We refer the reader to [3,4,9,10] and the references therein. Fundamental mathematical studies of the model were conducted in [1,2].

In our paper [7] the existence, uniqueness, and the continuity of the solution map $q \to y(q)$ over the set of the parameters $q \in P$ have been studied and newly derived in a unified framework. Furthermore, we have obtained the necessary conditions for the model's optimal parameters. In [8] the stability of the arch equations (1)-(3) has been studied under the assumptions of the symmetric initial shape and the time-independent symmetric load

$$u_0(x) = h\sin x, \quad \text{and} \quad p(x,t) = w\sin x. \tag{4}$$

The existence of the universal attractor for (1)-(3) with general initial and load functions was established in [6].

The so-called "snap-through" behavior of the arch refers to the arch changing its position from above the x axis to the one below it, or the other way around. Under certain combinations of the parameters of the model, the arch oscillates with or without a snap-through, and eventually settles at an equilibrium.

In [8] we introduced and studied critical parameter pairs (h,w), that separate the regions corresponding to the arch equilibrium position above or below the x axis. A small change in the values of the parameters for such a pair causes a significant change in the trajectory behavior, since the corresponding trajectories converge to distinct equilibria. In particular, at the critical pairs the equilibrium positions of the arch do not depend continuously on the parameters (h,w).

In [8] the effect of the initial velocity was not considered. That is, we assumed $v_0 = 0$. However it is important in applications to study the stability of (1)-(3)

with a nonzero initial velocity. In this paper we consider the case of $v_0 \neq 0$, as well as of a non-symmetric initial shape u_0 and the load p.

The arch behavior is strongly dependent on the damping effect. In this paper we take this effect into an account, and study the corresponding critical triples (h, w, γ). It is a complicated task, since an explicit expression for the solution for such triples does not seem to be possible. However, we were able to obtain some useful information via numerical simulations.

A common method for parameter estimation is the best fit to data approach, see [11]. Let $V(q),\ q = (h, w, \gamma)$ be the cost function defined by

$$V(q) = \|y(q) - z\|^2_{[0,T]}. \tag{5}$$

Here $y(q)$ is the solution of the model (1)-(3) corresponding to the triple of the parameters q, and z is the observation data. The norm is taken in an appropriate observation space.

To guarantee the existence of an optimal element q^* satisfying

$$V(q^*) = \min V(q), \quad q \in P,$$

we assume that the admissible set $P \subset \mathbb{R}^3$ is compact.

The continuity of the solution map $y(q) : P \to L^2[0, T]$ was established by us in [7]. However, it does not imply that the solutions depend continuously on the unbounded interval $0 \leq t < \infty$. Indeed, the critical pairs snap-through phenomenon described in [8] confirms that a small change in the system parameters q can lead to drastically different solution behavior as $t \to \infty$. In particular, the solutions may converge to distinct equilibria. In this paper we study how to conduct the parameter estimation for such a situation.

In Section 2 we examine the stability of a shallow arch with symmetric initial conditions and the load. In Section 3 these results are extended to non-symmetric conditions. In Sections 4 and 5 we describe our Parameter Estimation Algorithm for solving the estimation problem, and give results of the corresponding numerical experiments.

2. Stability for symmetric initial conditions and load

In this section we study stability of the system with the initial conditions and the load in the finite dimensional space $V_N = \text{span}\{\sin(nx),\ n = 1, 2, \ldots, N\}$. The central result established in [7] shows that given the initial conditions and the load in V_N, the solution y of (1)-(3) remains in V_N for all $t > 0$. We summarize this result in the following Theorem.

Theorem 2.1. *Let $u_0, v_0, p(t) \in V_N$, $t \geq 0$, and*

$$u_0 = \sum_{n=1}^{N} u_{0n} \sin(nx),\ v_0 = \sum_{n=1}^{N} v_{0n} \sin(nx),\ p\,(t) = \sum_{n=1}^{N} p_n(t) \sin(nx). \tag{6}$$

Then the solution y of (1)-(3) *is given by the finite series*

$$y(x,t) = \sum_{n=1}^{N} Y_n(t)\sin(nx),$$

where $Y_n = Y_n(t)$ are the solutions of the initial value problem

$$\ddot{Y}_n + \gamma\dot{Y}_n + n^4 Y_n + \frac{1}{4}n^2 Y_n\left(-\sum_{l=1}^{N} l^2 u_{0l}^2 + \sum_{l=1}^{N} l^2 Y_l^2\right) = n^4 u_{0n} + p_n, \tag{7}$$

$$Y_n(0) = y_{0n}, \quad \dot{Y}_n(0) = y_{1n}, \tag{8}$$

for $n = 1, 2, \ldots, N$, $t \geq 0$. Here $\dot{}$ and $\ddot{}$ denote the time derivatives.

Thus, in this case, the stability of (1)-(3) is determined by the stability of (7)-(8). Suppose that solutions Y_n approach an equilibrium as $t \to \infty$.

Denote

$$\hat{Y}_n = \lim_{t\to\infty} Y_n(t), \quad n = 1, \ldots, N. \tag{9}$$

In many applications the initial shape and the load are given by simple harmonic functions. Accordingly, in this section we assume that the load $p(x,t) = p(x)$ is time-independent, and

$$u_0(x) = h\sin x \quad \text{and} \quad p(x) = w\sin x, \tag{10}$$

where $h \geq 0$ and $w \in (-\infty, \infty)$. There are no restrictions on the initial velocity v_0, except that $v_0 \in V_N$.

Next Lemma shows that in this case the equilibrium $\hat{y}(x) = \lim_{t\to\infty} y(x,t)$ has a very simple form: it is at most the sum of two pure harmonics.

Lemma 2.2. *Suppose that* (10) *is satisfied, and $v_0 \in V_N$. Then the equilibrium shape $\hat{y}(x)$ satisfies either*

$$\hat{y}(x) = \hat{Y}_1 \sin x, \tag{11}$$

or

$$\hat{y}(x) = \frac{h+w}{1-n^2}\sin x + \hat{Y}_n \sin(nx) \quad \textit{for some } n \geq 2. \tag{12}$$

Furthermore, if $0 \leq h \leq 4$, then $\hat{y}(x) = \hat{Y}_1 \sin x$.

Proof. Equations for $\hat{Y}_n$, $n = 1, 2, \ldots, N$, follow from (7)-(8) by letting $\dot{Y}_n = \ddot{Y}_n = 0$:

$$\hat{Y}_1\left(4 - h^2 + \sum_{l=1}^{N} l^2 \hat{Y}_l^2\right) = 4(h+w), \tag{13}$$

$$\hat{Y}_n\left(4n^2 - h^2 + \sum_{l=1}^{N} l^2 \hat{Y}_l^2\right) = 0, \quad n = 2, 3, \ldots, N. \tag{14}$$

(i) Suppose that $\hat{Y}_n = 0$ for any $n = 2, \ldots, N$. Then we have (11).

(ii) Now assume that there is $k \geq 2$ such that $\hat{Y}_k \neq 0$. Then (14) implies $4k^2 - h^2 + \sum_{l=1}^{N} l^2 \hat{Y}_l^2 = 0$, and $-h^2 + \sum_{l=1}^{N} l^2 \hat{Y}_l^2 = -4k^2$. Substituting this into equations (14) gives

$$\hat{Y}_n(n^2 - k^2) = 0, \quad n = 2, \ldots, N.$$

Therefore $\hat{Y}_n = 0$ for all $n \neq k$, $2 \leq n \leq N$. For $n = 1$ we get $\hat{Y}_1(4 - 4k^2) = 4(h + w)$, and we get (12).

(iii) If $0 \leq h \leq 4$, then $4k^2 - h^2 + \sum_{l=1}^{N} l^2 \hat{Y}_l^2 > 0$, for any $n = 2, \ldots, N$, excluding the trivial case. Thus all $\hat{Y}_n = 0$ for any $n = 2, \ldots, N$, and we are back to the case (i). □

Lemma 2.2 studies the equilibrium for any $v_0 \in V_N$. Now we investigate the case $v_0 \in V_1$, i.e., $v_0(x) = v_{01} \sin x$, for the remaining of this section. Under this assumption Theorem 2.1 shows that the solution is given by $y = Y_1(t) \sin x$, where $Y_1 = Y_1(t)$, $t \geq 0$ satisfies

$$\ddot{Y}_1 + \gamma \dot{Y}_1 + \left(1 - \frac{h^2}{4}\right) Y_1 + \frac{1}{4} Y_1^3 - h - w = 0, \tag{15}$$

$$Y_1(0) = h, \quad \dot{Y}_1(0) = v_{01}. \tag{16}$$

The following Theorem 2.3 was established by us in [8, Section 3].

Theorem 2.3. *Suppose that u_0, p satisfy (10), and $v_0 \in V_1$. Define*

$$f(u) = u^3 + (4 - h^2)u - 4(h + w), \quad -\infty < u < \infty.$$

Let $\hat{u} \in \mathbb{R}$ be an equilibrium of the system (15), i.e., $\hat{u} = \hat{Y}_1 = \lim_{t \to \infty} Y_1(t)$. Then

(i) *If $\hat{u}$ is the unique root of equation $f(u) = 0$, then $\hat{u}$ is asymptotically stable.*

(ii) *If equation $f(u) = 0$ has three distinct roots $\hat{u}_1, \hat{u}_2, \hat{u}_3$ with $\hat{u}_1 < \hat{u}_2 < \hat{u}_3$, then $\hat{u}_1$ and $\hat{u}_3$ are asymptotically stable, and $\hat{u}_2$ is unstable.*

(iii) *If equation $f(u) = 0$ has three roots $\hat{u}_1, \hat{u}_2, \hat{u}_3$ such that $\hat{u}_1 = \hat{u}_2$, then the equilibrium $\hat{u}_3$ is asymptotically stable, and $\hat{u}_1$ is stable.*

Now we are going to illustrate the snap-through phenomenon, critical pairs and other concepts.

Example 2.4. Let $\gamma = 0.2$, and $h = 3$ be fixed. When $w = -3.387$, equation $f(u) = 0$ has three roots $\hat{u} = 0.316, 2.061$, and -2.377. The component $Y_1(t)$ converges to 2.061 as $t \to \infty$. Thus the arch equilibrium is $\hat{y}(x) = 2.061 \sin x$.

When $w = -3.388$, equation $f(u) = 0$ has three roots $\hat{u} = 0.317, 2.061$, and -2.378. Note that f is dependent of w. The component $Y_1(t)$ converges to -2.378 as $t \to \infty$, and the arch equilibrium is $\hat{y}(x) = -2.378 \sin x$.

Thus a small change in the value of the parameter w causes a significant change in the equilibrium position of the arch.

Figure 1 shows the graphs of the components $Y_1(t)$ corresponding to $w = -3.387$ and $w = -3.388$. The roots $\hat{u}$ are almost the same for $w = -3.387$ and

for $w = -3.388$, however the corresponding trajectory behavior is significantly different, since the trajectories converge to equilibria above and below the x axis. The trajectories diverge in their behavior around $t = 5$. When the function $Y_1(t)$ changes its sign, the arch snaps through the x axis.

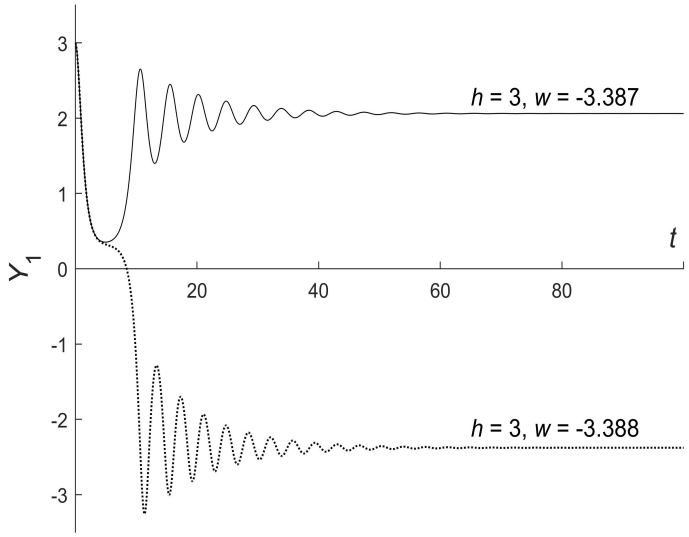

FIGURE 1. Components $Y_1(t)$ in Example 2.4

The snap-through phenomenon observed in Example 2.4 is dependent on the damping parameter γ. This is illustrated in Figure 2. We will call the triple of parameters $q = (h, w, \gamma)$, at which the position of the equilibria changes from above to below the x axis, a *critical triple*, and we call each such parameter a critical value.

In Example 2.4 parameters $q = (3, -3.388, 0.2)$ form a critical triple, and the numbers $3, -3.388, 0.2$ are the corresponding critical values.

In Figure we plot the critical parameters for various values of h and w. The figure shows the rectangle $[0, 4] \times [-8, 0]$ in the h-w plane subdivided into three open regions I, II and III. The regions are defined as follows. First, we draw the straight line $w = -h$, for $0 \le h \le 2$. Then draw two curves $w_+(h) = g(u_+(h))$ and $w_-(h) = g(u_-(h))$, for $2 \le h \le 4$, where

$$g(x) = \frac{1}{4}x^3 + \left(1 - \frac{h^2}{4}\right)x - h, \text{ and } u_\pm(h) = \pm\sqrt{\frac{1}{3}(h^2 - 4)}. \tag{17}$$

Clearly, all the curves meet at the same point $h = 2, w = -2$.

For all the points (h, w), $0 < h < 2$ we have $f'(u) = 3u^2 + (4 - h^2) > 0$. Therefore, for all such points, equation $f(u) = 0$ has a unique root $\hat{u}$, which is

the system equilibrium. By Theorem 2.3(i), the equilibrium is asymptotically stable. Rewrite equation $f(\hat{u}) = 0$, as $\hat{u}[\hat{u}^2 + (4 - h^2)] = 4(h + w)$. Since $h + w > 0$ in region I, we conclude that $\hat{u} > 0$ for $0 < h < 2$. On the other hand, in region II, below the line $w = -h$, we have $h + w < 0$, and $\hat{u} < 0$. Since the equilibrium is unique for $0 < h < 2$, there is no snap-through in region I and in region II for such vales of h. This is also seen in Figure 2.

A similar analysis for various points (h, w) for $h > 2$ in regions I and II shows that they may lead to the snap-through phenomena. The snap-through does not depend on γ for points in regions I and II for $2 < h < 4$. The snap-through phenomena is γ dependent in region III, because there are three equilibria whose signs are opposite, see [8, Section 3].

Next, let us draw the critical pairs (h, w) in region III. First, we notice that for all (h, w) satisfying $2 \le h \le 4$ and $w \le 0$ we have

$$\lim_{t\to\infty} Y_1(t; h, w, \gamma) = \hat{u} < h.$$

Indeed, we can rewrite equation $f(\hat{u}) = 0$ as

$$(\hat{u} - h)(\hat{u}^2 + h\hat{u} + 4) = 4w.$$

Suppose that $\hat{u} > 0$. Since $w < 0$, we conclude that $\hat{u} - h < 0$, and so $\hat{u} < h$. Now assume that $\hat{u} < 0$. Then either $\hat{u}^2 + h\hat{u} + 4 > 0$, or $\hat{u}^2 + h\hat{u} + 4 < 0$ is possible. If $\hat{u}^2 + h\hat{u} + 4 > 0$, then it is clear that $\hat{u} < h$, since $w < 0$. If $\hat{u}^2 + h\hat{u} + 4 < 0$, then $\hat{u} - h > 0$, i.e., $\hat{u} > h \ge 2$. However, this cannot happen since $\hat{u} < 0$ by the assumption.

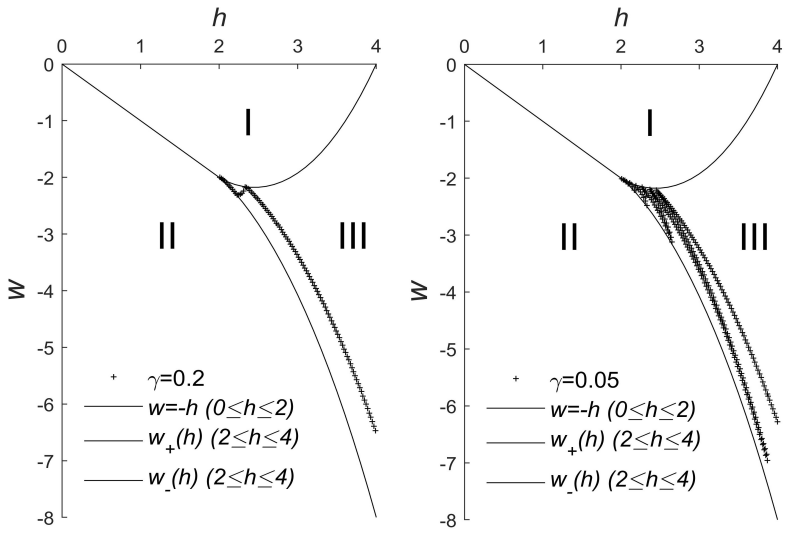

FIGURE 2. Critical pairs for $\gamma = 0.2$ and $\gamma = 0.05$

To summarize this discussion, $\lim_{t\to\infty} Y_1(t;h,w,\gamma) = \hat{u} < h$, when $0 \le h \le 4$ and $w \le 0$. Furthermore, either $\hat{u} < 0$, or $0 \le \hat{u} < h$. These cases can be distinguished by the curvature sign of the equilibrium shape. So, for the parameter pairs (h,w) the sign of $\hat{u}$ determines if the equilibrium is above or below the x axis. The critical pairs separate the regions where $\hat{u}$ have different signs.

The computations were carried out for $0 \le t \le 300$. Note that the computed set of critical pairs in Figure 2 looks like a zigzag line. The structure of the set of the critical pairs becomes more complex for smaller values of the air resistance coefficient γ. For $\gamma = 0.05$ the zigzag line acquires saw-tooth features.

3. Non-symmetric initial conditions and load

Now we consider non-symmetric initial conditions and the time-independent load $p(x,t) = p(x)$ given by

$$u_0 = h_1 \sin(x) + h_2 \sin(2x), \text{ and } p(x) = w_1 \sin(x) + w_2 \sin(2x), \tag{18}$$

where h_1, h_2 and w_1, w_2 are constants. The non-symmetric conditions are common because symmetric initial states can be changed by small perturbations.

Since $u_0, v_0 \in V_2$, and $p(t) \in V_2$ for any $t > 0$, we conclude by Theorem 2.1 that the solution is expressed by

$$y = Y_1(t)\sin(x) + Y_2(t)\sin(2x), \tag{19}$$

where $Y_1 = Y_1(t)$ and $Y_2 = Y_2(t)$ are the solutions of the system of ordinary differential equations

$$\begin{aligned}
&\ddot{Y}_1 + \gamma\dot{Y}_1 + \frac{1}{4}\left(4 - h_1^2 - 4h_2^2 + Y_1^2 + 4Y_2^2\right) Y_1 = h_1 + w_1,\\
&\ddot{Y}_2 + \gamma\dot{Y}_2 + \left(16 - h_1^2 - 4h_2^2 + Y_1^2 + 4Y_2^2\right) Y_2 = 16h_2 + w_2,\\
&Y_1(0) = h_1,\ Y_2(0) = h_2,\ \dot{Y}_1(0) = v_{01},\ \dot{Y}_2(0) = v_{02}.
\end{aligned}$$

Since this system depends on five parameters γ, h_1, h_2, w_1 and w_2, it is hard to analyze the stability similarly to the symmetric case considered in Section 2. Hence we are looking into how small perturbation parameters h_2, w_2 affect the trajectory Y_1, assuming that h_1, w_1 and γ are fixed.

The equilibrium components $\hat{Y}_1$ and $\hat{Y}_2$ are determined from the nonlinear system

$$\left(4 - h_1^2 - 4h_2^2 + \hat{Y}_1^2 + 4\hat{Y}_2^2\right)\hat{Y}_1 = 4(h_1 + w_1), \tag{20}$$

$$\left(16 - h_1^2 - 4h_2^2 + \hat{Y}_1^2 + 4\hat{Y}_2^2\right)\hat{Y}_2 = 16h_2 + w_2. \tag{21}$$

Equation (21) implies that the magnitude of $\hat{Y}_2$ is proportional to $16h_2 + w_2$. So, as long as $16h_2 + w_2$ is small, the behavior of the solution $y(x,t) = Y_1(t)\sin x + Y_2(t)\sin 2x$ is dominated by the component $Y_1(t)$.

Now we investigate how the regions I, II, and III, introduced in Example 2.4, and the corresponding critical pairs are changing when parameters h_1 and w_1 are perturbed by h_2 and w_2, satisfying (18).

Let $\delta = -h_2^2 + \hat{Y}_2^2$, and rearrange (20) to get

$$\left(4(1+\delta) - h_1^2 + \hat{Y}_1^2\right)\hat{Y}_1 = 4(h_1 + w_1). \tag{22}$$

Solutions of polynomial equations are continuously dependent on their coefficients. Therefore $\hat{Y}_1$ is continuously dependent on h_1, w_1 and δ in (22).

Repeating the analysis done for equation (17), while replacing 4 by $4(1+\delta)$, and $h = 2$ by $h_\delta = 2\sqrt{1+\delta}$. That is, $g(x)$ and $u_\pm(h)$ are changed to

$$g(x) = \frac{1}{4}x^3 + \left(1 + \delta - \frac{h^2}{4}\right)x - h, \text{ and } u_\pm(h) = \pm\sqrt{\frac{1}{3}(h^2 - 4 - 4\delta)}. \tag{23}$$

The following Example 3.1 shows that previously non-critical triple $(h_1, w_1, \gamma) = (3, -3.387, 0.2)$ turns into a critical triple by adding $h_2 = -0.02$.

Example 3.1. In this example the arch with non-symmetric initial shape and simple symmetric load is considered. Let us assume that $h_1 = 3$, $h_2 = -0.02$, $w_1 = -3.387$, $w_2 = 0$, the damping parameter is $\gamma = 0.2$, and the initial velocity is $v_0 = 0$.

Solving (20)-(21) for the equilibrium component $\hat{Y}_1$ gives the following three values

$$-2.3769,\ 0.3160 \text{ and } 2.0609.$$

On the other hand, if $\delta = 0$, the solutions for $\hat{Y}_1$ are

$$-2.3772,\ 0.3159 \text{ and } 2.0613.$$

Example 3.1 predicts that the larger the absolute value of δ is, the wider the region III becomes. In fact, Figure 4 shows that the regions I and II are reduced. On the other hand, the region III is expanded when $\delta = -0.1$, that is, if $h_\delta = 2\sqrt{0.9}$.

4. Parameter estimation problem

In this section we investigate the estimation problem for the arch system governed by equations (1)-(3). Our goal is to identify the model parameters from the observation of the system. In this study the problem is restricted to the time-independent load $p(t) = p \in V_N$. Thus

$$u_0(x) = \sum_{n=1}^{N} h_n \sin(nx),\ v_0(x) = \sum_{n=1}^{N} s_n \sin(nx),\ p(x) = \sum_{n=1}^{N} w_n \sin(nx). \tag{24}$$

By Theorem 2.1 the solution y of (1)-(3) is expressed by

$$y(x,t) = \sum_{n=1}^{N} Y_n(t)\sin(nx), \tag{25}$$

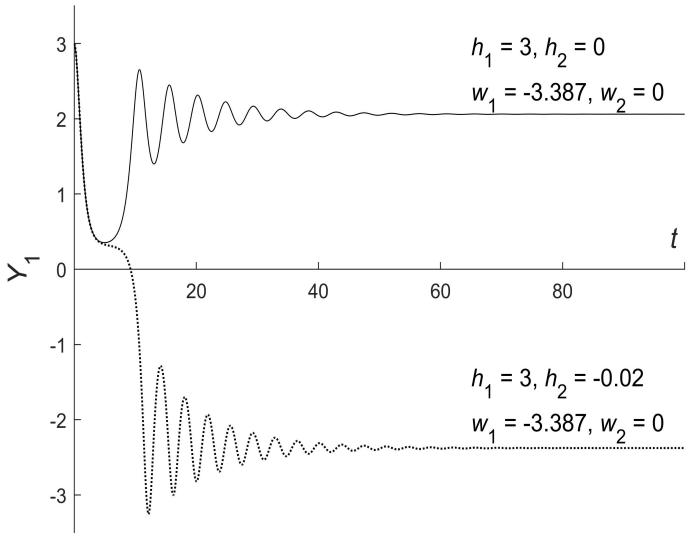

FIGURE 3. Component $Y_1(t)$ in Example 3.1

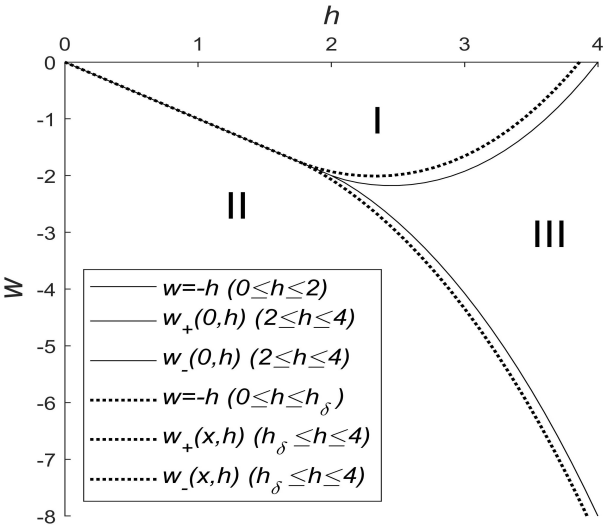

FIGURE 4. Change in regions I, II, and III, under small perturbations

where the component functions $Y_n = Y_n(t)$, $n = 1, 2, \ldots, N$ are the solutions of the initial value problem

$$\ddot{Y}_n + \gamma \dot{Y}_n + n^4 Y_n + \frac{1}{4} n^2 Y_n \sum_{j=1}^{N} j^2 (Y_j^2 - h_j^2) = n^4 h_n + w_n, \tag{26}$$

$$Y_n(0) = h_n, \quad \dot{Y}_n(0) = s_n, \tag{27}$$

for $n = 1, 2, \ldots, N$.

In this numerical study we will assume that $v_0 = 0$, thus $s_n = 0$ for all n. Let $\mathbf{h} = (h_1, h_2, \ldots, h_N) \in \mathbb{R}^N$, $\mathbf{w} = (w_1, w_2, \ldots, w_N) \in \mathbb{R}^N$, and $\gamma > 0$ be the unknown model parameters. Let $q = (\mathbf{h}, \mathbf{w}, \gamma) \in P \subset R^{2N+1}$, where the admissible set P is a closed box in $\mathbb{R}^{2N+1}$.

Assume that the system observation $z \in L^2(Q)$, $Q = [0, \pi] \times [0, T]$ is given. Introduce the objective function $V(q)$ by

$$V(q) = \int_0^T \int_0^\pi (y(x, t; q) - z(x, t))^2 dx dt, \tag{28}$$

where y is the solution of the system (1)-(3) with the parameters q.

The goal of the parameter estimation problem is to find an optimal set of parameters $q^* \in P$ satisfying

$$V(q^*) = \min_{q \in P} V(q). \tag{29}$$

In other words, $q^* = \text{argmin}_{q \in P} V(q)$.

We call q^* the optimal parameter and $y^* = y(q^*)$ the optimal state. It is proved in [7] that the solution map $q \to y(q)$, from P into $C([0, T], H_0^1[0, \pi])$ is continuous at any $q \in P$. Hence there is an optimal parameter $q^* \in P$, as P is closed and bounded in R^{2N+1}.

As we have already mentioned, the continuity $q \to y(q)$ of the solutions on any bounded interval $[0, T]$ does not imply the continuity of the map $q \to \hat{y}(q)$. This was illustrated in Section 2. A small change in the parameter values q near a critical pair causes drastically different solution behavior. Therefore, the direct minimization of the objective function $V(q)$ is unlikely to produce good results in such situations.

Our approach is to identify optimal parameters $q^* = (\mathbf{h}^*, \mathbf{w}^*, \gamma^*)$ in a sequential manner. First, we identify $\mathbf{h}^*$, then $\mathbf{w}^*$, and, finally, the damping coefficient γ^*. We will keep the q^* notation, even that such an optimal parameter set may not satisfy (29).

Parameter estimation algorithm.

(i) **Estimation of $\mathbf{h}^*$.**

By (24), $y(x, 0) = u_0(x) = \sum_{n=1}^N h_n \sin(nx)$. Thus we require

$$\mathbf{h}^* = \text{argmin}_{(h_1, \ldots, h_N)} \left\| \sum_{n=1}^N h_n \sin(nx) - z(x, 0) \right\|^2_{L^2[0,\pi]}.$$

The minimum is attained when $\mathbf{h}^*$ are the Fourier coefficients given by

$$h_n^* = \frac{2}{\pi} \int_0^\pi z(x, 0) \sin nx \, dx, \quad n = 1, \ldots, N.$$

(ii) **Estimation of $\mathbf{w}^*$.**

Let the observed arch equilibrium be $\hat{z}(x) = \lim_{t\to\infty} z(x,t)$. Since

$$\hat{y}(x) = \sum_{n=1}^{N} \hat{Y}_n \sin nx,$$

we identify the equilibrium components $\hat{Y}_n^*,\ n = 1,\dots,N$ from

$$\hat{\mathbf{Y}}^* = \operatorname{argmin}_{(Y_1,\dots,Y_N)} \left\| \sum_{n=1}^{N} Y_n \sin(nx) - \hat{z}(x) \right\|^2_{L^2[0,\pi]}.$$

Thus

$$\hat{Y}_n^* = \frac{2}{\pi} \int_0^\pi \hat{z}(x) \sin nx\, dx, \quad n = 1,\dots,N.$$

Observe from (26) that the equilibrium components $\hat{Y}_n^*$ satisfy the system

$$\left(4n^2 + \sum_{l=1}^{N} l^2((\hat{Y}_l^*)^2 - (h_l^*)^2)\right) n^2 \hat{Y}_n^* = 4(n^4 h_n^* + w_n^*), \quad n = 1,\dots,N. \tag{30}$$

Thus, since h_n^* and $\hat{Y}_n^*$ are already identified, we can find w_n^* from (30) by

$$w_n^* = \left(n^2 + \frac{1}{4}\sum_{l=1}^{N} l^2((\hat{Y}_l^*)^2 - (h_l^*)^2)\right) n^2 \hat{Y}_n^* - n^4 h_n^*, \quad n = 1,\dots,N. \tag{31}$$

(iii) **Estimation of $\boldsymbol{\gamma}^*$.**

With $h_n^*,\ w_n^*,\ n = 1,\dots,N$ already known, the minimization problem (29) is reduced to a one dimensional minimization with respect to γ. Thus, let

$$V(\gamma) = \|y(x,t;\hat{\mathbf{h}}^*, \hat{\mathbf{w}}^*, \gamma) - z(x,t)\|^2_{L^2(Q)}, \tag{32}$$

and

$$\gamma^* = \operatorname{argmin}_{\gamma>0} V(\gamma).$$

Remark. It was proved in [7, Section 7] that $V(\gamma)$ is differentiable in the interior of P. In particular, $\frac{dV}{d\gamma}$ exists at $\gamma^* \in \operatorname{int}(P)$. This implies that the optimal parameter γ^* is found either on the boundary of P of the admissible set, or in its interior *int* P, in which case we have $\frac{dV}{d\gamma}(\gamma^*) = 0$. Thus the gradient $\frac{dV}{d\gamma}(\gamma^*)$ can be used to identify γ^*. Practically, as illustrated in the next section, the objective function $V(\gamma)$ may have many local minima. Therefore global minimization methods are recommended.

5. Numerical experiments

For the purposes of numerical simulation we suppose that the arch motion is described by the system (1)-(3), and its solution $y(x,t)$ is approximated in the finite dimensional space V_N. Consistent with our stability analysis in previous sections, we conduct numerical experiments with $N = 1$ and $N = 2$.

Let the solution y be generated by the triple of parameters $q^* = (\mathbf{h}^*, \mathbf{w}^*, \gamma^*)$. We will write $y(x,t) = y(x,t;\mathbf{h}^*, \mathbf{w}^*, \gamma^*)$. To make the parameter estimation more realistic, we used noise contaminated observations $z(x,t)$ of the form

$$z(x,t) = y(x,t;\mathbf{h}^*, \mathbf{w}^*, \gamma^*) + \epsilon\eta(x). \tag{33}$$

Here $\eta(x)$ is a random variable uniformly distributed on interval $[-1,1]$, and the noise factor ϵ is a small constant. Accordingly, the initial condition becomes

$$z(x,0) = u_0(x,0;\mathbf{h}^*) + \epsilon\eta(x).$$

Recall, that we assume that $y_t(x,0) = v_0 = 0$.

Our goal is to find a triple $q_\epsilon^* = (\mathbf{h}_\epsilon^*, \mathbf{w}_\epsilon^*, \gamma_\epsilon^*)$, such that

$$V(q_\epsilon^*) = \min_{q\in P} V(q).$$

First we need to set the end time T_e, when the arch motion has almost stopped. This time was determined experimentally, depending on the parameter γ^*, from the stopping criterion

$$\|y(x,t) - y(x,t+\Delta t)\|^2_{L^2(Q)} \approx 0, \quad t \geq T_e$$

for a small $\Delta t > 0$.

Now let the optimal parameters $q_\epsilon^* = (\mathbf{h}_\epsilon^*, \mathbf{w}_\epsilon^*, \gamma_\epsilon^*)$ be determined by using the Parameter Estimation Algorithm described in Section 4.

Clearly, we expect to get a better parameter estimation in regions where the solution is more regular, i.e., away from the critical pairs. To understand this effect, consider the case $N = 1$, and $h = 3$. In Figure 5 we plot the equilibria $\hat{u}$ corresponding to various pairs $(w,\gamma) \in [-4.5,-2.5] \times (0, 0.5]$. The light gray points correspond to $\hat{u} > 0$, and the dark gray points correspond to $\hat{u} < 0$. The equilibrium values $\lim_{t\to\infty} Y_1(t) = \hat{u}$ are computed for $0 \leq t \leq 25000$.

Figure 5 shows that for $\gamma > 0.1$, there is just one corresponding critical pair, but for $0 < \gamma \leq 0.1$, the critical pairs do not exhibit a clear pattern. Another manifestation of this pattern can be seen from the behavior of the objective function $V = V(\gamma)$ defined in (32).

Let the observation $z(x,t) = y(x,t;\mathbf{h}^*, \mathbf{w}^*, \gamma^*)$ in (33) be generated by $q^* = (\mathbf{h}^*, \mathbf{w}^*, \gamma^*)$ with $\epsilon = 0$. According to the Parameter Estimation Algorithm, we estimate $\mathbf{h}^*$, and then $\mathbf{w}^*$. Then the value of γ^* is found by minimizing $V(\gamma)$.

For comparison purposes, function $V(\gamma)$ is normalized by its maximum, i.e., $V(\gamma) := V(\gamma)/\max_{0<\gamma\leq 1} V(\gamma)$. Function $V(\gamma)$ used for the estimation of γ^* in (32) depends on a normed space chosen to evaluate the discrepancy between the

data $z(x,t)$ and the solution $y(x,t;\hat{\mathbf{h}}^*,\hat{\mathbf{w}}^*,\gamma)$. For the numerical experiments in this section we selected the norm given by

$$\|u\|^2 = \sum_{j=1}^{5} \left| u\left(\frac{\pi j}{5}\right)\right|^2,$$

where $u \in C[0,\pi]$.

For $h^* = 3$ and $w^* = -2.3$, the graph of the function $V(\gamma)$ is shown in Figure 6 as a dash line. It is a regularly behaving function with a clearly defined unique minimum.

For $h^* = 3$ and $w^* = -1.3$, the graph of the function $V(\gamma)$ is shown in Figure 6 as a dotted line. It coincides with the graph of $V(\gamma)$ for $h^* = 3$, and $w^* = -0.3$, shown as an alternated long and short dash line. The functions also have a clearly defined unique minimum.

The behavior of $V(\gamma)$ is very different for $h^* = 3$, and $w^* = -3.3$, which is shown as a solid line. In this case $q^* = (3, -3.3, 0.01)$ is a critical point. We see that the graph of $V(\gamma)$ is oscillating, having many local minima, which makes the identification process challenging and imprecise.

Example 5.1. In this example the identification results for $N = 1$ and various levels of the noise factor ϵ, are shown in Tables 1, 2, and 3. The optimal parameters are given by $h^* = 3$, $w^* = -1.3$, with $\gamma^* = 0.01$, $\gamma^* = 0.05$, and $\gamma^* = 0.1$. The stopping times were chosen to be $T_e = 1877$, $T_e = 376$, and $T_e = 188$ corresponding to $\gamma^* = 0.01, 0.05$, and 0.1.

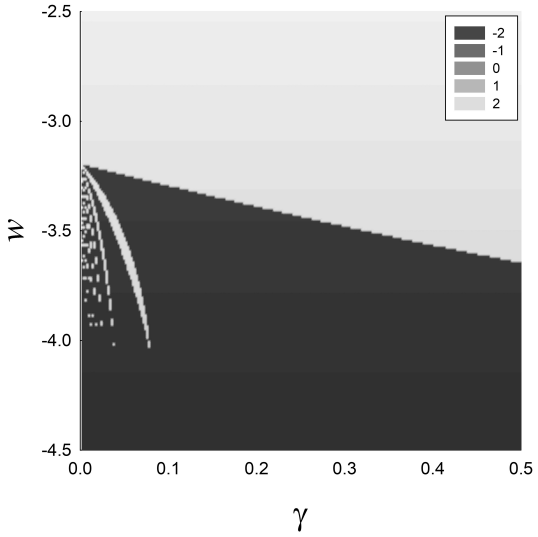

FIGURE 5. Equilibria $\hat{u} > 0$ (light gray), and $\hat{u} < 0$ (dark gray), for various pairs (w,γ), $N = 1$, $h = 3$.

Whenever ϵ is small, the suggested Parameter Estimation Algorithm finds good optimal parameters q_ϵ^* for small γ^*. But when ϵ becomes bigger, the estimates worsen, especially for γ_ϵ^*, as can be seen in Table 1. Table 3 shows that when γ^* is sufficiently large, the Parameter Estimation Algorithm provides good identification for all considered noise levels.

TABLE 1. Estimation for $\gamma^* = 0.01$

ϵ	h_ϵ^*	w_ϵ^*	γ_ϵ^*	$V(\gamma_\epsilon^*)$
0.000	3.00000	-1.29989	0.01004	$4.797e-08$
0.001	3.00023	-1.30000	0.00973	$3.090e-06$
0.005	3.00056	-1.29981	0.00900	$2.513e-05$
0.010	2.99946	-1.29132	0.00755	$1.724e-04$
0.050	2.98771	-1.21648	0.00091	$4.292e-03$

TABLE 2. Estimation for $\gamma^* = 0.05$

ϵ	h_ϵ^*	w_ϵ^*	γ_ϵ^*	$V(\gamma_\epsilon^*)$
0.000	3.00000	-1.29990	0.04998	$1.734e-08$
0.001	2.99987	-1.30071	0.05052	$3.372e-06$
0.005	3.00013	-1.29466	0.04861	$6.792e-05$
0.010	3.00186	-1.33290	0.05874	$1.109e-03$
0.050	2.98409	-1.25458	0.06278	$3.090e-03$

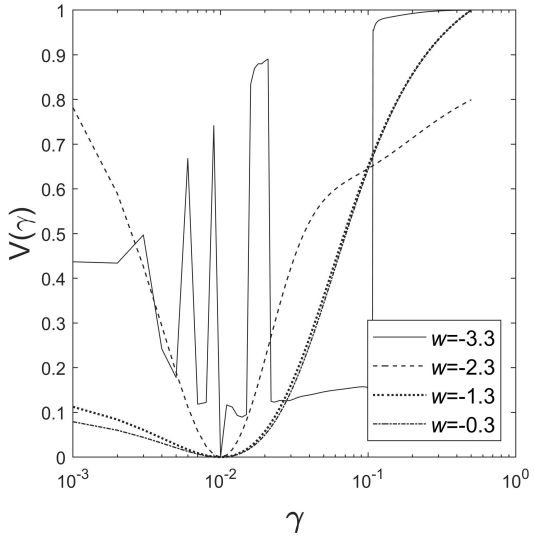

FIGURE 6. Function $V(\gamma) := V(\gamma)/\max V(\gamma)$ for $h^* = 3$, and various values of w^*.

TABLE 3. Estimation for $\gamma^* = 0.1$

ϵ	h^*_ϵ	w^*_ϵ	γ^*_ϵ	$V(\gamma^*_\epsilon)$
0.000	3.00000	−1.30009	0.10036	$2.628e-07$
0.001	2.99987	−1.30014	0.10049	$1.853e-06$
0.005	2.99929	−1.29430	0.09909	$3.740e-05$
0.010	2.99925	−1.28340	0.09614	$3.714e-04$
0.050	2.97843	−1.17046	0.09424	$4.096e-03$

Example 5.2. The identification results for $N = 2$ are shown in Table 4. Accordingly, the parameters $\mathbf{h}^*$, and $\mathbf{w}^*$ are given by vectors in V_2, i.e., they have two components, see (18).

The optimal parameters are given by $\mathbf{h}^* = (3, 0.2)$, $\mathbf{w}^* = (-1.3, -0.2)$, $\gamma^* = 0.01$. The stopping time was chosen to be $T_e = 1871$.

The results show that for $N = 2$, the Parameter Estimation Algorithm is much more sensitive to noise, as compared to the case of $N = 1$.

TABLE 4. Estimation for $\gamma^* = 0.01$

ϵ	h^*_ϵ	w^*_ϵ	γ^*_ϵ	$V(\gamma^*_\epsilon)$
0.000	3.00000	−1.29990	0.01007	$8.055e-08$
	0.20000	−0.20003		
0.000	3.00003	−1.30078	0.01067	$7.499e-06$
	0.19973	−0.19121		
0.000	2.99971	−1.30300	0.01250	$1.928e-04$
	0.19936	−0.16785		
0.000	3.00121	−1.29986	0.00664	$3.036e-04$
	0.20205	−0.23370		
0.000	2.99018	−1.29719	0.01555	$7.762e-03$
	0.21081	−0.55812		

6. Conclusions

Stability of solutions and parameter estimation for the system (1)-(3) were investigated for sinusoidal initial shapes and loads. To summarize, if the initial conditions u_0, v_0 and the load $p(t)$ belong to the finite-dimensional space V_N, the solution $y(t)$ remains in V_N for any $t \geq 0$.

With these assumptions and a time-independent load p, the static solution (i.e., the equilibrium) $\hat{y}(x)$ was shown to be expressed as $\hat{y}(x) = \hat{Y}_1 \sin x + \hat{Y}_n \sin(nx)$ for some n. In the special case $u_0 = h \sin x$, $p = w \sin x$, and $v_0 \in V_1$, the static solution is shown to be $\hat{y}(x) = \hat{Y}_1 \sin x$, and its stability was completely analyzed.

We have introduced the notion of critical parameter sets, separating the regions where the initial data imply convergence to different equilibria. A

numerical study of critical values $\mathbf{h}, \mathbf{w}$, dependent on the damping parameter γ, was conducted.

The Parameter Estimation Algorithm for the identification of system's parameters from its observation was proposed, and its efficiency has been analyzed numerically. Numerical experiments show good results for small noise levels, as well as for the initial parameter sets away from critical values. A study of the identification near the critical values shows that the difficulties can be traced to the erratic behavior of the objective function $V(\gamma)$.

References

[1] J. M. Ball, *Initial-boundary value problems for an extensible beam*, J. Math. Anal. Appl. **42** (1973), 61–90. https://doi.org/10.1016/0022-247X(73)90121-2

[2] ———, *Stability theory for an extensible beam*, J. Differential Equations **14** (1973), 399–418. https://doi.org/10.1016/0022-0396(73)90056-9

[3] Q. Bi and H.H. Dai, *Analysis of non-linear dynamics and bifurcations of a shallow arch subjected to periodic excitation with internal resonance*, J. Sound Vibration **233** (2000), no. 4, 553–567.

[4] J. Chen and Y. Li, *Effects of elastic foundation on the snap-through buckling of a shallow arch under a moving point load*, ntern. J. Solids Structures **43** (2006), no. 14, 4220–4237.

[5] E. Emmrich and M. Thalhammer, *A class of integro-differential equations incorporating nonlinear and nonlocal damping with applications in nonlinear elastodynamics: existence via time discretization*, Nonlinearity **24** (2011), no. 9, 2523–2546. https://doi.org/10.1088/0951-7715/24/9/008

[6] S. Gutman and J. Ha, *Uniform attractor of shallow arch motion under moving points load*, J. Math. Anal. Appl. **464** (2018), no. 1, 557–579. https://doi.org/10.1016/j.jmaa.2018.04.025

[7] S. Gutman, J. Ha, and S. Lee, *Parameter identification for weakly damped shallow arches*, J. Math. Anal. Appl. **403** (2013), no. 1, 297–313. https://doi.org/10.1016/j.jmaa.2013.02.047

[8] J. Ha, S. Gutman, S. Shon, and S. Lee, *Stability of shallow arches under constant load*, Intern. J. Non-Linear Mech. **58** (2014), 120–127.

[9] W. Lacarbonara and G. Rega, *Resonant non-linear normal modes. II. Activation/orthogonality conditions for shallow structural systems*, Internat. J. Non-Linear Mech. **38** (2003), no. 6, 873–887. https://doi.org/10.1016/S0020-7462(02)00034-3

[10] J. Lin and J. Chen, *Dynamic snap-through of a laterally loaded arch under prescribed end motion*, Intern. J. Solids Structures **40** (2003), no. 18, 4769–4787.

[11] J.-L. Lions, *Optimal control of systems governed by partial differential equations*, Translated from the French by S. K. Mitter. Die Grundlehren der mathematischen Wissenschaften, Band 170, Springer-Verlag, New York, 1971.

Semion Gutman
Department of Mathematics
University of Oklahoma
Norman, Oklahoma 73019, USA
Email address: sgutman@ou.edu

Junhong Ha
School of Liberal Arts
Korea University of Technology and Education
Cheonan 31253, Korea
Email address: hjh@koreatech.ac.kr

Sudeok Shon
School of Architectural Engineering
Korea University of Technology and Education
Cheonan 31253, Korea
Email address: sdshon@koreatech.ac.kr